SPECIAL ISSUE PAPER

European Journal of **Soil Science** WILEY

Potential erodibility of semi-arid steppe soils derived from aggregate stability tests

Moritz Koza[1] | **Julia Pöhlitz**[1] | **Aleksey Prays**[2] | **Klaus Kaiser**[2] |
Robert Mikutta[2] | **Christopher Conrad**[1] | **Cordula Vogel**[3] |
Tobias Meinel[4] | **Kanat Akshalov**[5] | **Gerd Schmidt**[1]

[1]Department of Geoecology, Institute of Geosciences and Geography, Martin Luther University Halle-Wittenberg, Halle (Saale), Germany

[2]Soil Science and Soil Protection, Institute of Agricultural and Nutritional Sciences, Martin Luther University Halle-Wittenberg, Halle (Saale), Germany

[3]Institute of Soil Science and Site Ecology, Technische Universität Dresden, Tharandt, Germany

[4]TOO Amazone Kazakhstan, Amazonen-Werke H. Dreyer SE & Co. KG, Hasbergen, Germany

[5]Soil and Crop Management, Barayev Research and Production Center for Grain Farming, Shortandy, Kazakhstan

Correspondence
Moritz Koza, Institute of Geosciences and Geography, Martin Luther University Halle-Wittenberg, Von-Seckendorff-Platz 4, 06120 Halle (Saale), Germany.
Email: moritz.koza@geo.uni-halle.de

Funding information
Bundesministerium für Bildung und Forschung

Abstract

Erosion is a severe threat to the sustainable use of agricultural soils. However, the structural resistance of soil against the disruptive forces steppe soils experience under field conditions has not been investigated. Therefore, 132 topsoils under grass- and cropland covering a large range of physico-chemical soil properties (sand: 2–76%, silt: 18–80%, clay: 6–30%, organic carbon: 7.3–64.2 g kg^{-1}, inorganic carbon: 0.0–8.5 g kg^{-1}, pH: 4.8–9.5, electrical conductivity: 32–946 μS cm^{-1}) from northern Kazakhstan were assessed for their potential erodibility using several tests. An adjusted drop-shatter method (low energy input of 60 Joule on a 250-cm^3 soil block) was used to estimate the stability of dry soil against weak mechanical forces, such as saltating particles striking the surface causing wind erosion. Three wetting treatments with various conditions and energies (fast wetting, slow wetting, and wet shaking) were applied to simulate different disruptive effects of water. Results indicate that aggregate stability was higher for grassland than cropland soils and declined with decreasing soil organic carbon content. The results of the drop-shatter test suggested that 29% of the soils under cropland were at risk of wind erosion, but only 6% were at high risk (i.e. erodible fraction >60%). In contrast, the fast wetting treatment revealed that 54% of the samples were prone to become "very unstable" and 44% "unstable" during heavy rain or snowmelt events. Even under conditions comparable to light rain events or raindrop impact, 53–59% of the samples were "unstable." Overall, cropland soils under semi-arid conditions seem much more susceptible to water than wind erosion. Considering future projections of increasing precipitation in Kazakhstan, we conclude that the risk of water erosion is potentially underestimated and needs to be taken into account when developing sustainable land use strategies.

Highlights

- Organic matter is the important binding agent enhancing aggregation in steppe topsoils.
- Tillage always declines aggregate stability even without soil organic carbon changes.
- All croplands soil are prone to wind or water erosion independent of their soil properties.
- Despite the semi-arid conditions, erosion risk by water seems higher than by wind.

1 | INTRODUCTION

Drylands cover 41% of the Earth's land surface and are particularly vulnerable to human activities and climate change (Reynolds et al., 2007). Large areas in the semi-arid steppe regions of Central Asia are currently under severe threat of increasing soil erosion due to intense agriculture and increasingly extreme climate conditions (Mirzabaev et al., 2016; Reyer et al., 2017; Robinson, 2016). Central Asia's most important grain producer is Kazakhstan, with 84.5 Mio hectares of potential agricultural land (FAO, 2012). However, 25.5 Mio hectares are already affected by wind erosion and 1 Mio hectare by water erosion due to missing vegetation cover and unsustainable land use (Almaganbetov & Grigoruk, 2008; Cerdà et al., 2009). In northern Kazakhstan, approximately, 23 Mio hectares of native grassland were converted into cropland during the largest global ecosystem conversion in the twentieth century ("Virgin Lands Campaign") (Frühauf et al., 2020; Prishchepov et al., 2020). Strong wind gusts over 40 m s^{-1} favour wind erosion, and extreme snowmelts during spring or heavy rain events during summer cause erosion by water (FAO, 2012; Muñoz Sabater, 2019; Wang et al., 2020; WHO, 2012). Under the dry continental climate, 66% of the annual precipitation occurs as snowfall and severe thunderstorms in the summer are often linked to flash floodings (FAO, 2012; Harris et al., 2020; Zepner et al., 2021). Climate models indicate that the risk of soil erosion will increase in northern Kazakhstan in future (Li et al., 2020; Teixeira et al., 2013). Extreme temperature episodes enhance draughts (Teixeira et al., 2013; Wang et al., 2020; WHO, 2012), and in response to increasing rainfall duration, magnitude, and intensity, the risk of water erosion (Duulatov et al., 2021).

The susceptibility of soil to erosion depends mainly on the stability of its structure against mechanical stress, which is directly linked to the stability of aggregates (Diaz-Zorita et al., 2002; Le Bissonnais, 2016, 1996b). In turn, the formation of aggregates is linked to soil properties that promote interactions among primary particles, such as rearrangement, flocculation, and cementation (Amézketa, 1999; Bronick & Lal, 2005; Diaz-Zorita et al., 2002; Six et al., 2004). For example, higher soil clay content typically increases aggregate stability, although swelling of clay during wetting (Bronick & Lal, 2005) can promote the breakdown of aggregates. Especially in semi-arid regions, soluble salts can contribute to the aggregation and disaggregation of primary particles (Amézketa, 1999; Fernández-Ugalde et al., 2011; Virto et al., 2011). Besides inorganic constituents, organic matter is an important binding agent (Jarvis et al., 2012; Tisdall & Oades, 1982) but its effect on aggregate stability varies considerably depending on soil type and external factors such as climate and land use (Six et al., 2004). For instance, tillage is the agricultural land use practice that most deteriorates aggregate stability (Amézketa, 1999; Bronick & Lal, 2005; Diaz-Zorita et al., 2002; Six et al., 2004). However, the mutual effects of agriculture and soil properties on aggregate stability and potential erodibility on steppe soils have not been comprehensively addressed.

Methods for determining aggregate stability often vary in the mechanical stress used and complicate the comparability between studies and field conditions (Almajmaie et al., 2017; Amézketa, 1999; Diaz-Zorita et al., 2002). As there is no single standardised procedure available to rank the soils' structural resistance against the disruptive forces of wind and water, it is necessary to combine different methods to assess erosion susceptibility (Kemper & Rosenau, 2018). The adjusted drop-shatter method with a low energy input of 60 Joule can be applied to estimate the stability of dry soil against weak mechanical forces, such as saltating particles striking the surface, causing the suspension of soil particles during a wind erosion event (Diaz-Zorita et al., 2002; Hadas & Wolf, 1984; Larney, 2007; López et al., 2007; Shao, 2008). The three wetting tests proposed by Le Bissonnais (2016,

1996b) are usually applied to estimate aggregate stability in terms of water erosion under various wetting conditions and energies: the fast wetting treatment assesses the breakdown during heavy rain or snowmelt, the slow wetting treatment is used to simulate the effect of light rain, and the wet shaking treatment addresses mechanical breakdown by raindrop impact (Le Bissonnais, 2016, 1996b). This uniform framework is considered the best approach to assess aggregate stability over a wide range of potentially erosive conditions and has been applied successfully worldwide (Bartoli et al., 2016).

In this study, we applied the four aggregate stability tests described above to explore the resistance of aggregates of steppe soils against different mechanical stresses to assess the potential erodibility by wind and water. We assessed the extent and relevant factors of aggregation by studying soils with a wide range of physico-chemical properties sampled at seven sites across northern Kazakhstan. Additionally, we compared soils from cropland with grassland at each site to single out the effect of tillage on aggregate stability under given soil conditions. Ultimately, our objectives were (i) to determine the main soil properties enhancing aggregation, (ii) to explore the effect of tillage (grassland vs. cropland), and (iii) to assess the potential erodibility of cropland by investigating the consequences of mechanical stress on aggregate stability similar to disruptive forces by wind and water.

2 | MATERIALS AND METHODS

2.1 | Study area

The study area is located in the north of Kazakhstan and connects the central with the east-central part of the Eurasian steppe (Figure 1). The dry continental climate at the seven test sites is characterised by comparable annual mean temperatures (2.5–3.8°C) and precipitation (299–352 mm) based on weighted interpolation (1989–2018) (Harris et al., 2020; Zepner et al., 2021). Sites 1 and 2 are located close to Kokshetau, Sites 3, 4, and 5 close to Astana, Site 6 is located south of Ekibastuz, and Site 7 east of the Irtysh close to the border of Russia and the Kulunda steppe (Figure 1). Soils at Sites 1 and 2 are Haplic Chernozems, those at Site 5 are Calcic Kastanozems, and at Sites 3, 4, 6, and 7 are Haplic Kastanozems (FAO, 2014). Kastanozems correspond in the national classification system to Dark Chestnut Soils (Stolbovoi, 2000; Uspanov et al., 1975). A meteorological station (ecoTech GmbH, Bonn, Germany) with a multisensor (WXT536, Vaisala GmbH, Hamburg, Germany) at a two-meter height was installed on Site 1 to monitor real weather conditions in the study area, including temperature, wind speed, and precipitation.

2.2 | Soil sampling

Soil samples were collected in May and June 2019. Each site was represented by one native grassland and up to six cropland plots. Native grassland plots were used for occasional grazing but had never been cultivated. The typical vegetation on grassland was dominated by Stipa (*Stipa capillata* L.), Volga fescue (*Festuca valesiaca Schleich. ex Gaudin*), and shrubs (*Artemisia spp.*). Grassland plots were conscientiously selected for representing an initial situation to reference the effect of tillage at each site. All croplands were under reduced tillage, which is the most common practice in the study area. Croplands were managed for spring wheat, the most common crop.
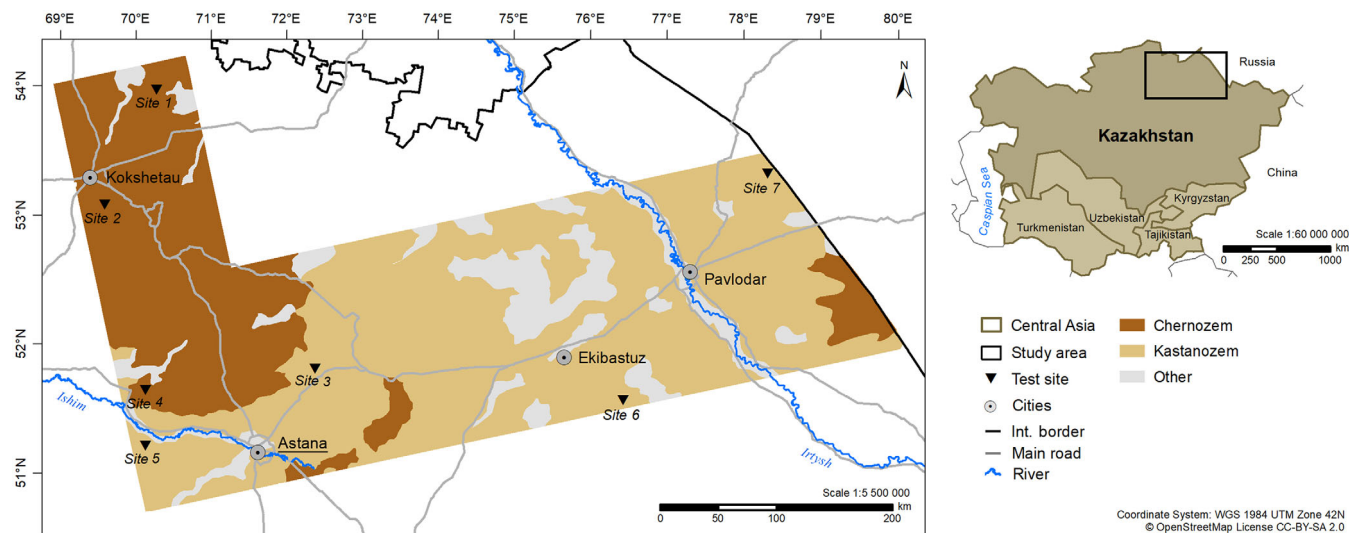

FIGURE 1 Location of the study area with seven test sites and dominant soil types in northern Kazakhstan (Uspanov et al., 1975)
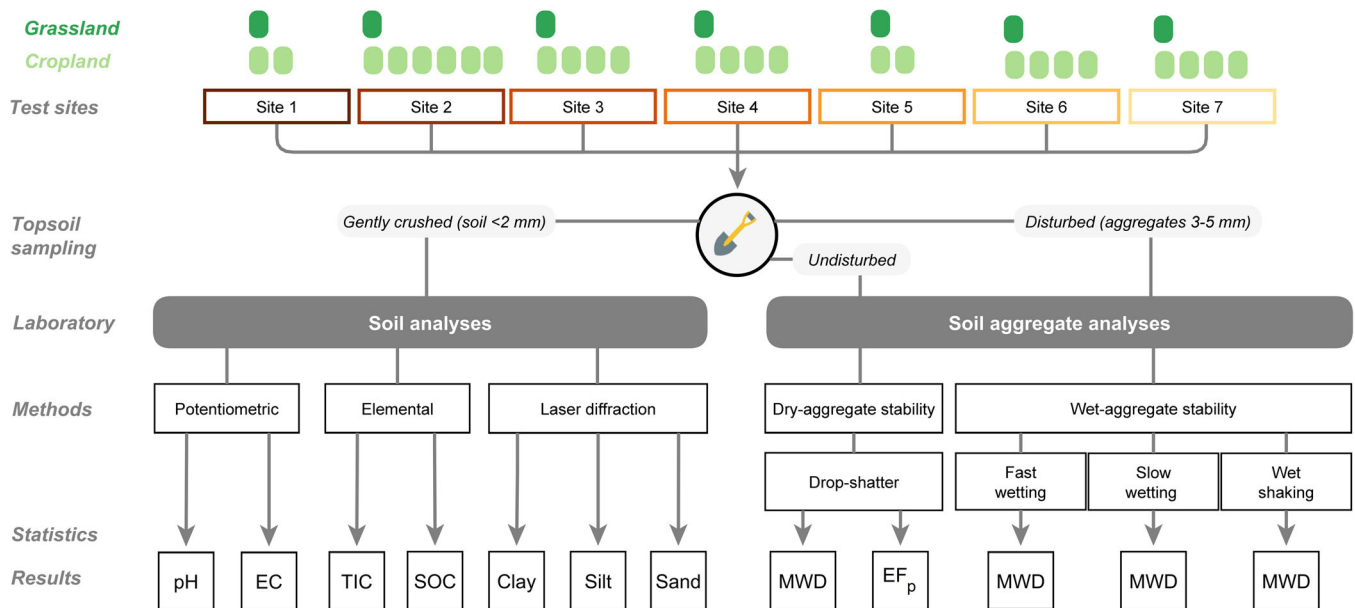
FIGURE 2 Study design with applied materials and methods. Abbreviations: EC, electrical conductivity; TIC, total inorganic carbon; SOC, soil organic carbon; MWD, mean weight diameter; and EF_p, potential erodible fraction

In total, seven native grassland and 26 continuous cropland plots were sampled. Despite being managed similarly, cropland plots differed slightly in terms of management practices, machinery used, and field characteristics, such as different ages after conversion and crop history (Table A1). Topsoil samples were collected from 0–5 cm depth, most susceptible to erosion (Zachar, 1982). Each plot was sampled at four randomly selected spots ($n = 33$ plots $\times 4$ spots $= 132$) (Figure 2). Soil cores of 250 cm³ (diameter $= 80$ mm, height $= 50$ mm) were taken and transferred into plastic bags for transportation. Before conducting soil analyses, they were air-dried at 40°C for 24 h, gently crushed, and dry-sieved to <2-mm with loose organic material removed. For analysing dry-aggregate stability, 132 undisturbed soil blocks of 250 cm³ (width $= 50$ mm, length $= 100$ mm, height $= 55$ mm) and for wet-aggregate stability, 132 boxes (width $= 50$ mm, length $= 100$ mm, height $= 55$ mm) with soil aggregates broken apart by hand from clods were collected ($n = 132$ spots $\times 3$ sample types $= 396$).

dispersing 2 g of ground sample material in 50 ml 2 M HCl at 50°C and subsequent detection of the released CO_2 (soliTIC modul interfaced to the varioMax Cube, Elementar Analysensysteme GmbH, Langenselbold, Germany). The soil organic carbon (SOC) content was calculated by subtracting TIC from total carbon. Soil texture was evaluated by a laser diffraction analyser (Helos/KR, Sympatec GmbH, Clausthal Zellerfeld, Germany) equipped with a 60 W sonotrode for wet dispersion (Quixel, Sympatec GmbH, Clausthal Zellerfeld, Germany). Before texture analyses, soil was pre-treated with 30% hydrogen peroxide (H_2O_2) (Koza et al., 2021) and 0.05 M sodium pyrophosphate ($Na_4P_2O_7 \cdot 10\ H_2O$) to remove organic matter and support dispersion (ISO 13320, 2009). Analyses were carried out in duplicates with 2–3 g soil for 20 s (20–30% obscuration rate). Single-particles were described mathematically by the Fraunhofer theory (Green & Perry, 2007; ISO 13320, 2009). Particle size classes of >2, 2–50, and 50–2000 μm were used for assigning soil texture (Soil Science Division Staff, 2017).

2.3 | Soil analyses

The pH and electrical conductivity (EC) were measured in distilled water at a 1-to-2.5 soil-to-solution (weight-to-volume) ratio. Total carbon and total nitrogen were analysed by dry combustion at 950°C (varioMax Cube, Elementar Analysensysteme GmbH, Langenselbold, Germany). Total inorganic carbon (TIC) was analysed by

2.4 | Soil aggregate analyses

2.4.1 | Dry-aggregate stability

Drop-shatter
An adjusted drop-shatter method (Hadas & Wolf, 1984; Marshall & Quirk, 1950) was used to estimate the stability of dry soil against weak mechanical forces during

saltation bombardment. The energy applied onto the undisturbed soil blocks of 250 cm³ was 60 J derived from Equation 1:

$$E^* = m \times g \times h \times n \qquad (1)$$

where E^* is the cumulative energy J imparted on the soil sample, and m the mass defined by a 6-kg metal plate dropped onto the sample once (n) from a height (h) of 0.1 m with the gravitation acceleration (g) of 9.81 m s^{-2}.

Fragment size distribution: The dry-aggregate size distribution after mechanical impact was obtained by dry sieving. Therefore, a horizontal sieving apparatus (Analysette 3, Fritsch GmbH, Idar-Oberstein, Germany) with eight different sieves (8, 5, 3, 2, 0.85, 0.5, 0.25, and 0.05 mm) was used for 60 s and an amplitude of 1 mm. Sieving time was restricted to prevent fragmentation due to abrasion (Cole, 1939). The dry-aggregate size distribution after drop-shatter was described by the mean weight diameter (MWD), which is commonly used as a stability index (Nimmo & Perkins, 2002), as calculated based on Equation 2:

$$\mathrm{MWD} = \sum_{i=1}^{n} \overline{x}_i w_i \qquad (2)$$

where x_i is the mean diameter of the size fraction [mm], and w_i is the proportion of the total sample retained on the sieve. The upper limit was estimated by doubling the size of the largest sieve (Larney, 2007). The derived midpoint (12 mm) was used as an MWD for samples that did not disintegrate under the impact of 60 J.

The erodible fraction, a simple index for potential wind erosion (Larney, 2007), can be calculated as the weight percent of aggregates <0.84 mm after separating fragments (Chepil, 1953). Sieving can be obtained with a rotary (Chepil, 1962) or a comparable horizontal sieve (López et al., 2007). A European standard sieve size of 0.85 mm can also be used (Leys et al., 1996). The potential erodible fraction (EF$_p$) was calculated after drop-shatter and dry sieving with an 0.85 mm horizontal sieve using Equation 3:

$$\mathrm{EFp} = \frac{W < 0.85}{\mathrm{TW}} \times 100\% \qquad (3)$$

where $W < 0.85$ is the weight [g] of <0.85-mm aggregates, and TW is the initial weight [g] of the total sample. In general, soils with an EF >60% are considered critical (Anderson & Wenhardt, 1966) and indicate a high risk of wind erosion (Larney, 2007). In contrast, an EF <40% indicates a negligible risk of wind erosion. (Leys

et al., 1996). However, according to the erodibility classification by Shiyatyi (1965), as cited by Zachar (1982) and López et al. (2007), an EF >50% already indicates a high risk of wind erosion. Still, they consider EF <40% to indicate substantial resistance to wind erosion.

2.4.2 | Wet-aggregate stability

A unified framework with three treatments was used to analyse aggregate stability against water disruption. The treatments were conducted on 3–5 mm aggregates collected previously by dry sieving. If gravel was visually present within the 3–5 mm aggregate fraction, samples were omitted to avoid misleading results. Immediately before each test, aggregates were oven-dried at 40°C for 24 h and cooled in a desiccator (ISO 10930, 2011).

Fast wetting
The fast wetting treatment, also called "slaking", corresponds to a heavy rain event and is recommended for comparing soils containing high amounts of organic carbon (Le Bissonnais, 2016, 1996b), such as the Chernozems in the study area. As the first step, 4 g of aggregates were gently immersed in a 250-ml beaker filled with 50 ml deionised water. After 10 min, the supernatant was decanted, and aggregates were carefully transferred to a 0.05-mm sieve immersed in ethanol to determine fragment size distribution.

Slow wetting
The slow wetting treatment corresponds to a light rain event on soil aggregates. A fine-pored cellulose sponge (height 3.7 cm) was placed in a flat vessel for pre-wetting. Distilled water was added to a height of 3 cm. A filter paper (DP 5893125, Hanemühle Fine Art GmbH, Dassel, Germany) was placed on the sponge and saturated. Then, 4 g aggregates were arranged on the filter paper. Thus, capillary flow slowly wetted aggregates for 30 min before being transferred to a 0.05-mm sieve immersed in ethanol to determine fragment size distribution.

Wet shaking
The mechanical breakdown by shaking after pre-wetting treatment corresponds to the breakdown by raindrop impact. Aggregates were pre-wetted with 95% ethanol to remove air from aggregates. Then, 4 g of aggregates were gently immersed in a 250-ml beaker filled with 50 ml 95% ethanol. After 10 min, the ethanol was removed with a pipette. The soil aggregates were then carefully transferred to a 250-ml Erlenmeyer flask filled with 200 ml deionised water. Then, the flask was shaken for 1 min at 20 rounds per minute using an overhead shaker (GFL

3040, Gesellschaft für Labortechnik mbH, Burgwedel, Germany). After letting the soil fragments settle for 30 min, the water was removed. The aggregates were carefully transferred to a 0.05-mm sieve immersed in ethanol to determine fragment size distribution.

Fragment size distribution

Two successive steps were completed to measure fragment size distribution after each treatment. First, aggregates transferred to a 0.05-mm sieve immersed in ethanol (95%) were moved five times in circles by hand to separate fragments >0.05 mm from fragments <0.05 mm. Ethanol (95%) was used to reduce further breakdown and was recycled by filtering. Second, fragments >0.05 mm were dried at 40°C for 48 h and then sieved. A horizontal sieving apparatus with six different sieves (2, 1, 0.5, 0.2, 0.1, and 0.05 mm) was used to separate fragments. Dry sieving was carried out for 60 s with an amplitude of 0.5 mm. The measured mass percentage of each size fraction was used to calculate the MWD (Equation 2) for each breakdown mechanism. A gravel correction is necessary to avoid misinterpretation of results if gravel content is between 10% and 40% (ISO 10930, 2011). Since samples with gravel were avoided initially, the content was always less than 10%. Still, if gravel was retained on the 2 mm sieve, it was weighted additionally, and the MWD was calculated without gravel.

According to Le Bissonnais (2016, 1996b), the stability of aggregates can be classified based on the following MWD values: >2 mm "very stable" aggregates, 1.3–2.0 mm "stable" aggregates, 0.8–1.3 mm "medium" stable aggregates, 0.4–0.8 mm "unstable" aggregates, and <0.4 mm as "very unstable" aggregates. "Very unstable" aggregates indicate a "high permanent risk," "unstable" aggregates indicate "frequent" risk, and "medium" stable aggregates suggest "variable" risk depending on climatic parameters. The risk of water erosion is "limited" for "stable" aggregates and "very low" for "very stable" aggregates (ISO 10930, 2011).

2.5 | Statistical analyses

RStudio (Version 4.1.2, RStudio Team) was used for statistical analyses and graphs (R Core Team, 2020). All measured properties from each plot were tested for normal distribution (Shapiro-Wilk test) and variance homogeneity (Levene's test), followed by variance analyses (one-way ANOVA). Tukey's HSD (honestly significant difference) test was performed to identify mean group values that are significantly different (Table A1). For all soils, texture triangles (Figure 3) were illustrated with the "soiltexture" package (Moeys, 2018) and the principal component analysis (PCA) (Figure 4) with "factoextra" (Kassambara & Mundt, 2020). Pearson's correlation was performed between aggregate stability indicators and all measured soil properties for all samples and individual sites (Table A2). Significances of correlations are indicated at a level of $p < 0.05$. Subsequently, a correlation matrix was generated with "corrplot" (Taiyun & Simko, 2021) for all soils (Figure 5). The aggregate stability indicators from grassland and cropland were tested for normal distribution (Shapiro–Wilk test) and variance homogeneity (Levene's test). Afterward, Welch's t-test (unequal variance t-test) was applied for each site due to unequal sample groups (Figure 6).

All soils and cropland soils from each site were tested for variance homogeneity (Levene's test), followed by the rank-based Kruskal-Wallis test to compare sites and to assess erosion risk across the study area. The Dunn's test was used as post hoc for the non-parametric pairwise multiple comparisons (Figure 7). Further, variance analyses (one-way ANOVA) and Tukey's HSD test were conducted for comparing the three different wet-aggregate stability indicators on all sites (not shown).

3 | RESULTS

3.1 | Soil properties and aggregate stabilities in the study area

The pH of all soil samples was 7.3 ± 0.8 (mean $\pm$ SD), the EC 261.9 ± 158.3 μS cm^{-1}, the C:N ratio 11.6 ± 1.2, the TIC content 1.7 ± 2.3 g kg^{-1}, and the SOC content 23.9 ± 10.9 g kg^{-1}. In the study area, more than half of the samples had a silt loam texture ($n = 87$); the remaining soils were classified as either loam ($n = 26$), sandy loam ($n = 14$), silty clay loam ($n = 8$), or loamy sand ($n = 1$). Overall, the samples of the seven sites covered a wide range of sand (2–76%), silt (18–80%), and clay contents (6–30%). A textural gradient occurred from Sites 1–3 with low sand content to Sites 6–7 with high ones (Figure 3a). The SOC contents decreased with declining clay and silt contents (Figure 3b). The average MWD of aggregates determined by drop-shatter was 6.6 ± 3.0 mm and EF$_p$ accounted for $34.2 \pm 15.3\%$. Indicators of wet-aggregate stability showed an MWD after fast wetting of 0.6 ± 0.5 mm, after slow wetting of 1.0 ± 0.6 mm, and after wet shaking of 1.0 ± 0.5 mm (Table A1). Aggregate stability was highest in soils from Site 1 and lowest in soils from Site 7, independent of the mechanical stress applied.

3.2 | Relationship between soil properties and aggregate stability

The two main principal components of the PCA describe 69.5% of the data variability. The PCA shows a strong
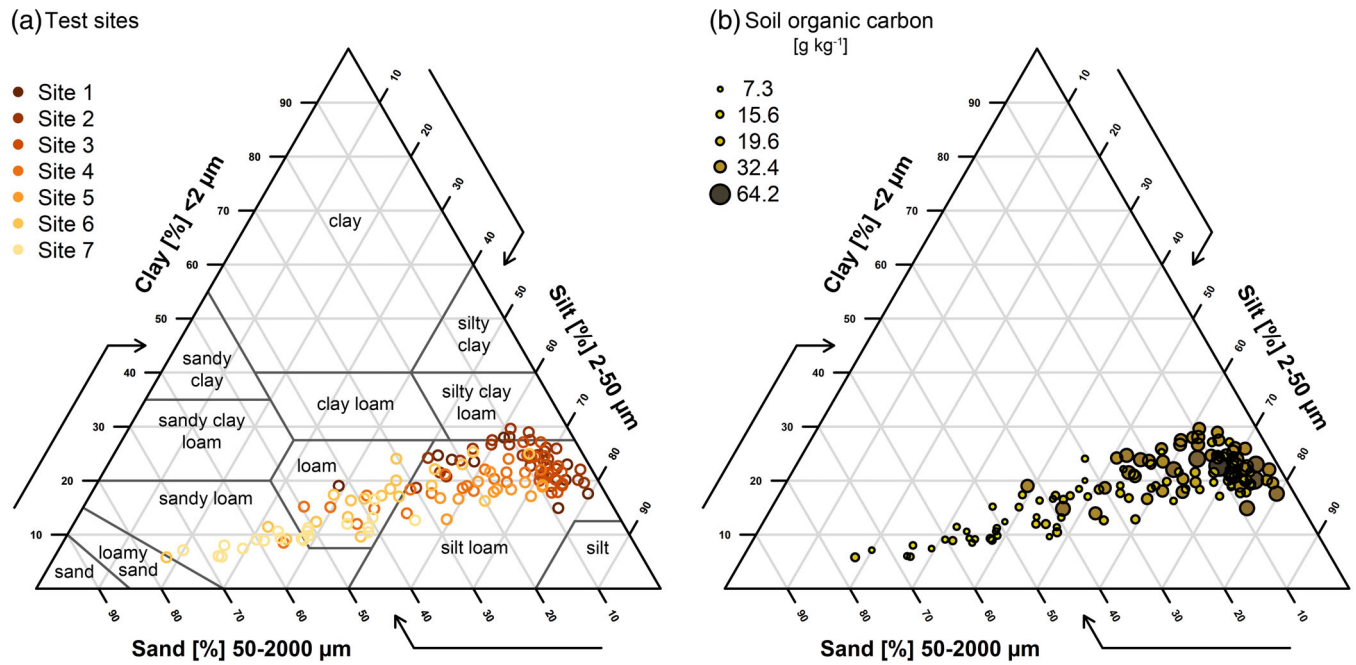
(a) Test sites

- Site 1
- Site 2
- Site 3
- Site 4
- Site 5
- Site 6
- Site 7

(b) Soil organic carbon
[g kg⁻¹]

- 7.3
- 15.6
- 19.6
- 32.4
- 64.2

FIGURE 3 Soil texture triangles define textural classes (a) (Soil Science Division Staff, 2017) of all sites and soil organic carbon contents in combination with clay, silt, and sand contents (b). It shows the decrease of SOC content with increasing sand content. The legend is classified according to minima, first quartile, median, third quartile, and maxima of soil organic carbon contents
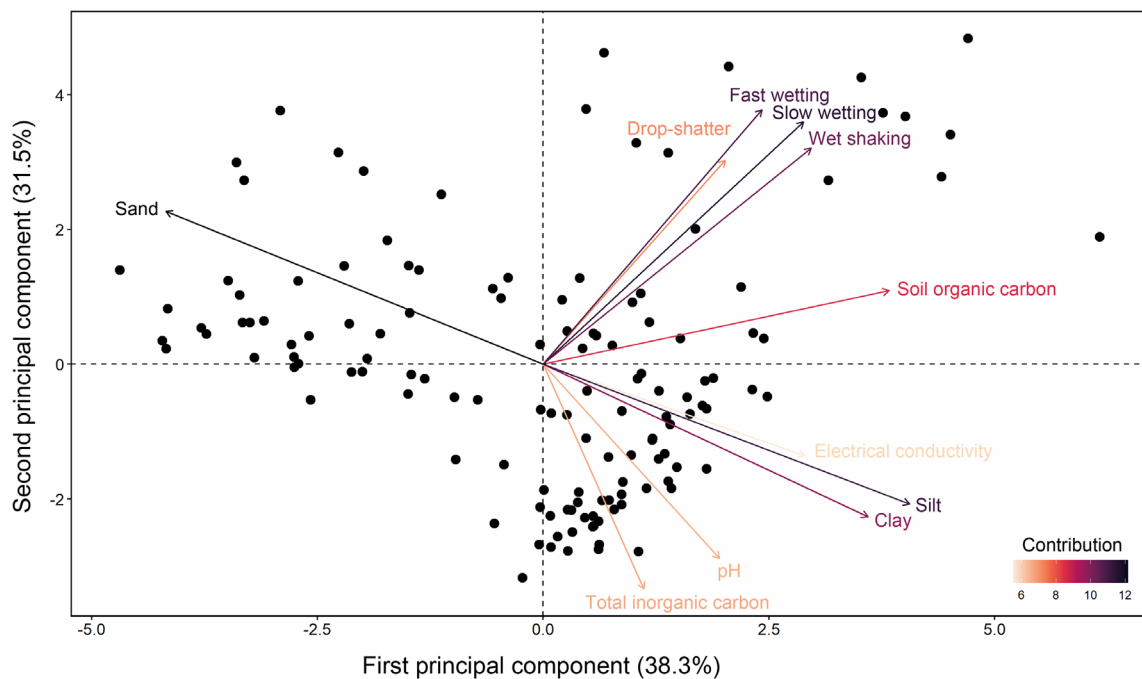
FIGURE 4 Biplot of the principal component analysis (PCA) indicates a strong relationship between different aggregate stability indicators due to eigenvectors close to each other. The closest relationship between all stability indicators and soil organic carbon can also be observed. Texture, soil organic carbon, and aggregate stability indicators strongly contribute to the principal components indicated by arrow length

positive correlation between the different aggregate stability indicators. The eigenvectors of drop-shatter, fast wetting, slow wetting, and wet shaking form a small angle (Figure 4), indicating a similar relationship between the various aggregate stability indicators and soil properties. However, the correlation among the three

wet-aggregate stability indicators ($r = 0.87$–0.92) was higher than those with the stability indicator determined by drop-shatter ($r = 0.50$–0.59) (Figure 5). The PCA eigenvector of SOC suggests a positive relationship to the aggregate stability indicators, showing a strong relationship (Figure 4), which is in line with correlation analysis (Figure 5). A moderate correlation was observed between aggregate stability determined by drop-shatter and SOC ($r = 0.51$). The correlation coefficients were similar for SOC and aggregate stability determined by fast wetting ($r = 0.42$), slow wetting ($r = 0.49$), and wet shaking ($r = 0.43$). In addition, a negative and very weak correlation was observed between TIC and all aggregate stability indicators (Figure 5). Both PCA and bivariate correlation analysis showed that other soil properties had only a minor impact on soil aggregate stability.

Noteworthy, the relationships between soil properties and aggregate stability indicators varied strongly between sites (Table A2). While the correlation between SOC and aggregate stability is strong at Site 1, 3, and 5, and moderate at Site 2, correlations were nonsignificant at Sites 4, 6, and 7. The SOC contents on Site 6 (13.3 ± 3.2 g kg^{-1}) and 7 (14.1 ± 2.9 g kg^{-1}) were the lowest in the study area (Table A3), but this does not apply to Site 4 (25.3 ± 10.3 g kg^{-1}), where SOC contents were similar to those at Site 3 (21.2 ± 4.1 g kg^{-1}) and 5 (19.8 ± 5.4 g kg^{-1}). Additionally, the silt content at Site 1 ($64.3 \pm 11.5\%$) affected all four aggregate stability indicators ($r = 0.67$–0.78). However, at Site 2, the silt content was similar ($65.4 \pm 7.6\%$) to that at Site 1 but only a weak, nonsignificant correlation with aggregate stability could be observed. Further, TIC had a moderate negative impact on aggregate stability at Site 3 and a strong negative at Site 5, with both sites being well above the average TIC content of all sites (Site 3: 4.7 ± 0.9 g kg^{-1}, Site 5: 5.0 ± 3.6 g kg^{-1}; all sites: 1.7 ± 2.3 g kg^{-1}; Table A3). The correlation between TIC and the wet-aggregate stability was higher than for the dry-aggregate stability determined by drop-shatter (Table A2).

## 3.3 | Comparison of aggregate stability and soil properties on grassland and cropland

Mean values of aggregate stability indicators were higher for grassland than cropland at all sites (Table A3), showing a decline in aggregate stability from grassland to cropland. The decline was 14–62% for the drop-shatter, 65–77% for the fast wetting treatment, 39–69% for the slow wetting, and 38–70% for the wet shaking, respectively (Figure 6). Overall, mean values of SOC were higher for grassland than for cropland (Table 2). Comparing grass- with cropland, SOC decreased between 1–30% (Figure 6) due to tillage. A significant decrease could only be observed at Sites 1 and 3 (Figure 6; Table A1). The TIC and clay content were generally higher on cropland than on grassland (Table A3).

3.4 | Comparison of erosion risk on cropland under different mechanical stresses

Mechanical stress applied to cropland soils with drop-shatter revealed a mean MWD of 5.8 ± 2.4 mm and an average EF_p of $33.9 \pm 15.7\%$, suggesting that all croplands are prone to wind erosion. Mean values obtained by drop-shatter for Sites 3–7 with lower SOC contents showed significantly higher EF_p than Sites 1–2, indicating a higher susceptibility to wind erosion (Figure 7). About 71% of the soils showed EF_p of <40% (negligible risk of wind erosion), while the remaining 29% of soils had values above and are, therefore, at risk of wind erosion. However, only about 6% of the study soils, all located at Sites 3–6, showed very high EF_p values of >60%, indicating a "high" risk of wind erosion (Anderson & Wenhardt, 1966). Results obtained for all sites indicate that fast wetting was significantly more disruptive than the other wet-aggregate stability treatments (Figure 8a–c). Comparing the different wet-aggregate stability treatments revealed that the decline MWD values increased with increasing overall stability (Figure 8a,b). In general, the fast wetting treatment caused lower average MWD values (0.4 ± 0.2 mm) than slow wetting (0.8 ± 0.3 mm) and wet shaking (0.8 ± 0.3 mm) (Table A3). This means 98% of the soils of the study area were at a "frequent" (44%) or "permanently high" (54%) risk of water erosion upon heavy rain or snowmelt events. Especially, Sites 3, 5, and 7 showed significantly lower MWD values than other sites, indicating a "permanently high" risk of water erosion. As simulated by the slow wetting treatment, even a light rain event revealed "frequent" erosion risk for 59% of the samples. Especially, Sites 3–7, where SOC is below 30 g kg^{-1}, seem prone to water erosion at relatively moderate disruption by wetting. The wet shaking treatment showed similar results ("frequent" risk on 53% of the samples) as the slow wetting treatment (Figure 7; Figure 8a,b). Gentle rain and raindrop impact caused the highest risk of water erosion on Site 7, similar to the fast wetting treatment. Hence, the overall soil erodibility by water, independent of wetting energy applied, is the highest on Site 7, where the lowest SOC and clay content were measured in the study area.

FIGURE 5 Correlation matrix reveals significant linear correlations ($p < 0.05$) between soil organic carbon, texture, and the four aggregate stability indicators determined by the drop-shatter, fast wetting, slow wetting, and wet shaking test. The positive correlation between aggregate stability indicators and soil organic carbon indicates that organic is the most important binding agent, enhancing aggregation
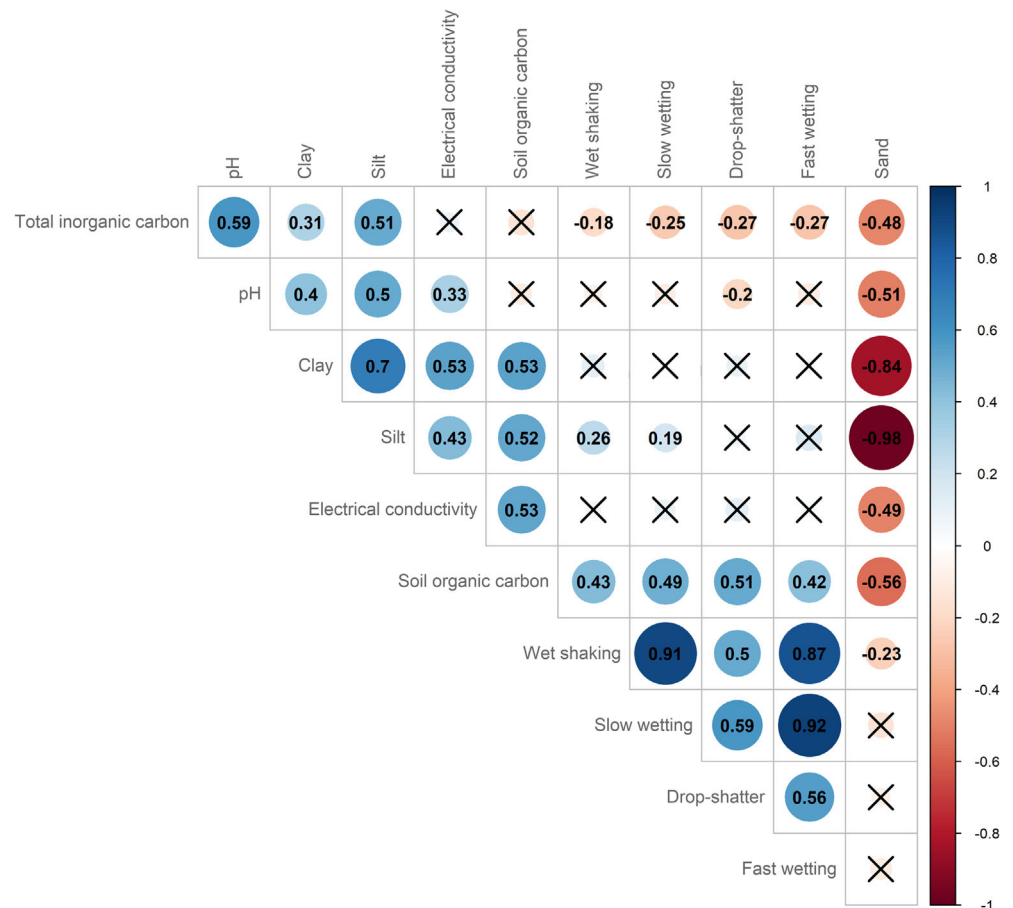
4 | DISCUSSION

4.1 | Soil properties promoting aggregation in steppe soils

A significant positive relationship was observed between SOC and aggregate stability in the study area, indicating organic matter as an important binding agent. This result aligns with a previous study (Koza et al., 2021), and underlines the importance of organic matter, which contributes decisively to aggregate stability in the semi-arid steppe, similar to other climatic zones (e.g., Eynard et al., 2005; Malobane et al., 2021; Rahmati et al., 2020; Xue et al., 2019). Overall, aggregate stability increased with increasing SOC content, independent of the disruptive force applied. However, no strong relationship between aggregate stability and SOC could be detected on Site 4, even though SOC did not differ from Sites 3 and 5. This reflects the possibility of additional factors that influence aggregate stability, such as biotic factors (e.g., plant species, roots, microbial activity, termites) or soil management (e.g. fertiliser, crop history) (Amézketa, 1999; Bronick & Lal, 2005). The lack of relationships between measured soil properties and aggregate stabilities on Sites 6 and 7 suggests that these soils did not contain enough

binding agents (e.g., SOC and clay) to effectively support aggregate formation (Bronick & Lal, 2005). While it is generally accepted that inorganic carbon favours soil aggregation (Bronick & Lal, 2005; Six et al., 2004), the effect may depend on clay content and the particle size of calcium carbonates (Dimoyiannis et al., 1998; Le Bissonnais, 1996a). Our results revealed a negative correlation between TIC and aggregate stability. Surprisingly, inorganic carbon seemed less relevant as a binding agent in northern Kazakhstan, even in soils with high TIC content. However, this agrees with a previous study from that region, where dissolving carbonates for texture analysis did not cause dispersion of aggregates (Koza et al., 2021). Dimoyiannis et al. (1998) observed that silt-sized carbonates negatively influenced wet-aggregate stability in Greek agricultural soils. One reason might be that soils low in clay content and with silt-sized calcium carbonates feature the typical instability of silty soils (Le Bissonnais, 1996a).

4.2 | Effect of tillage on aggregate stability and soil properties

Our results are consistent with previous studies, showing that aggregate stability was lower for cropland than
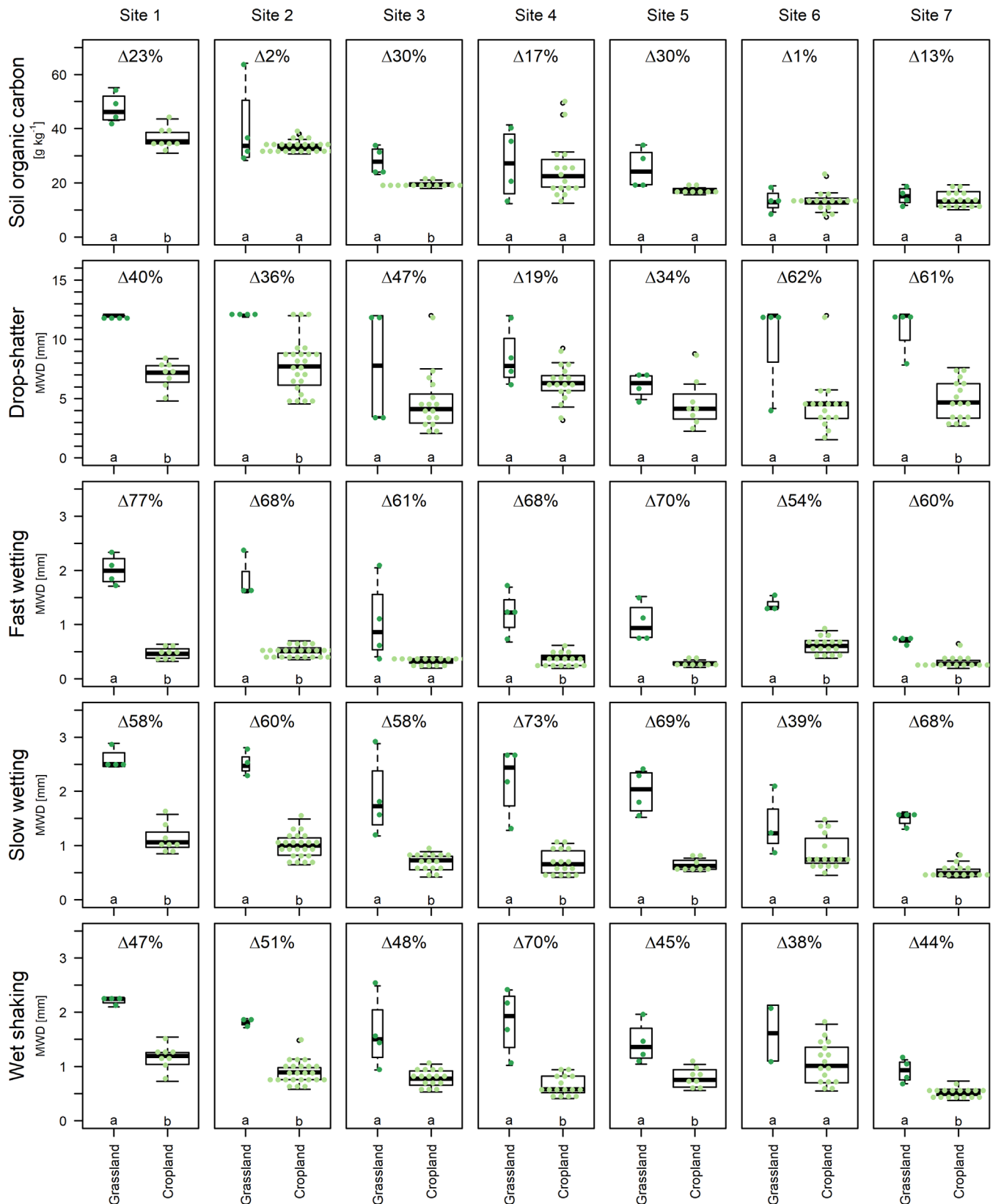
FIGURE 6 Boxplots for all sites show the soil organic carbon content for grassland (dark green dots) and cropland soils (light green dots) and the lower mean weight diameters (MWD) for all aggregate stability indicators. Every dot represents the measurement of one individual soil sample. The number of samples defines the width of each boxplot, and numbers above the boxplot indicate the relative decline from grassland to cropland. Different lower case letters indicate significant differences ($p < 0.05$) between the two dominant land use types

FIGURE 7 Erosion risk as determined from four aggregate stability tests similar to disruptive forces soils experiences under field conditions. Boxplots show that cropland is more vulnerable to the disruptive forces of water than wind. Especially, the severe breakdown of aggregates during heavy rain or snowmelt events cau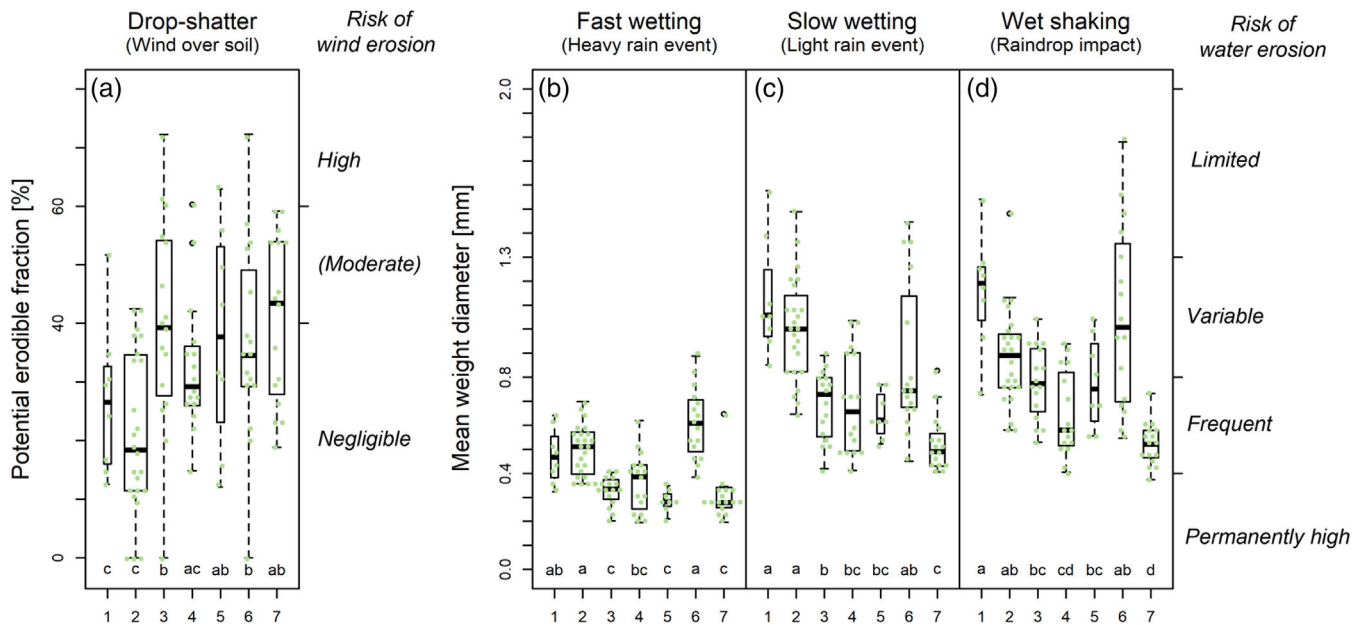ses a high risk of water erosion. The number of samples defines the width of each boxplot. Different lower case letters show significant differences ($p < 0.05$) between sites for each stability indicator

grassland (e.g. Six et al., 1998). The breakdown of soil structure by tillage is due to mechanical stress repeatedly applied to soil (Amézketa, 1999). Six et al. (1998) showed that frequently disrupted soils contain less intra-aggregate particular organic matter and less stable micro-aggregates within macroaggregates. Additionally, cropland soils rewet much faster than grassland soils because of their lower organic matter content (Caron et al., 1996; Six et al., 2004). Higher organic matter contents typically increase the water drop penetration time (Chenu et al., 2000), thus reducing overall soil wettability (Woche et al., 2017). Therefore, the disruptive force by wetting during wet–dry cycles outweighs the stabilising effect of drying, particularly for cropland soils, causing an overall decrease in aggregation (Six et al., 2004). In addition, the studied grassland soils had extensive visible roots, similar to observations in the prairies of North America (Beniston et al., 2014). Roots physically stabilise the soil structure and thus, account for the higher aggregate stability of grassland soils as determined by the drop-shatter method (Tisdall & Oades, 1982).

Similar patterns in aggregate stability of cropland vs grassland soils have been observed in the Kulunda steppe of southern Russia (Bischoff et al., 2016; Illiger et al., 2019; Schmidt et al., 2020). Bischoff et al. (2016) also noted a decrease in SOC contents and aggregate stability, determined by wet-sieving, from grassland to cropland across different steppe types (forest, typical, dry). Mikhailova et al. (2000) compared Chernozems from the

Kursk region of Russia under native grassland with a continuously cropped plot and observed a relative decline in SOC content of 38% (grassland = 55.3 ± 2.7 g kg^{-1}; cropland = 34.5 ± 1.5 g kg^{-1}). This result is similar to the substantial SOC loss due to tillage at Sites 1 and 3 but disagrees with findings at Site 2 with similar SOC content. In summary, aggregation decreases with decreasing SOC content, but tillage further worsens the structural stability of soils. Our study suggests to use agricultural practices that support soil organic matter accumulation and minimising the disruptive impact of tillage (e.g., by direct seeding, mulching, or catch crops) because they provide the highest potential for reducing the vulnerability of steppe soils against erosion.

Apart from soil degradation due to declining aggregate stability and mostly decreasing SOC contents, cropping also affected TIC and clay contents of the studied soils. The higher TIC contents in cropland than in grassland soils can be explained by tillage-induced erosion of topsoil layers. Typically, topsoils are more depleted in TC than the less weathered deeper horizons. Removal of surface soil exposes deeper material and thus, results in apparent increases in topsoil TIC contents (Suarez, 2017). The higher clay content in the cropland soils suggests depletion of particles >2 μm, likely by wind erosion. Even though tillage does not directly influence soil texture, previous studies have shown that wind redistributes particles in semi-arid grasslands (Larney, 2007; Li et al., 2009), especially in the absence of vegetation

(Gyssels et al., 2005). Since clay has a higher threshold against aerodynamic forces due to more efficient cohesion of particles (Shao, 2008), wind erosion causes preferential removal of coarser particles and subsequent clay enrichment in topsoils of croplands.

4.3 | Assessment of potential erodibility on cropland by mechanical stress

Measuring aggregate stability with different methods revealed that all cropland soils in the study area are principally prone to erosion by wind and water. This supports the view of erosion as the major factor in soil degradation of croplands in Central Asia (Hamidov et al., 2016; Mirzabaev et al., 2016). The aggregate size distribution of dry soil is a major factor influencing wind erosion (Skidmore et al., 1994). Applying mechanical stress with the drop-shatter method on dry soil to assess the erodibility by wind showed that almost all soils are potentially erodible. Results of EF_p from Kazakhstan are well in line with measurements from semi-arid Argentinean Pampas (EF = 39.5%) using a rotary sieve on similar soils (Colazo & Buschiazzo, 2010). The risk of wind erosion in northern Kazakhstan is moderate, as 29% of the soils are prone, and 71% are expected to resist wind erosion. Still, soils low in SOC exhibit a higher EF_p, suggesting an increased risk of wind erosion in the study area, particularly once SOC is further lost by less sustainable agricultural practices. Yet, wind erosion depends on additional environmental factors such as micro-topographic (microrelief, vegetation cover, etc.), macro-topographic conditions (windbreaks, etc.), and especially climate (wind abundance and speed, temperature, rainfall, etc.) (Shao, 2008). In Central Asia, the wind erosion rate is mostly related to wind speed ($r^2 = 0.31–0.72$), followed by temperature ($r^2 = 0.06–0.66$), and precipitation ($r^2 = 0.16–0.56$). Due to the strong correlations between erosion rate and climate factors, northern Kazakstan will likely be highly sensitive to climate change (Li et al., 2020).

In our study area, wind occurred predominantly (98.5%) at wind speeds of 3.4 ± 2.1 m s^{-1} in the year after soil sampling (observed period: 07/01/2019–06/30/2020), with wind gusts reaching up to 21.5 m s^{-1} at 2 m height. However, assuming that the aerodynamic drag and lift overcome the retarding forces of the surface particles at speeds of 4–6 m s^{-1} in 30 cm above the soil surface (Scheffer et al., 2016), potential wind erosion events are rather rare. Considering the logarithmic wind profile (Shao, 2008) and estimated surface roughness of 0.005 m for fallow with negligible vegetation (Wieringa, 1992), wind speeds must exceed 5.9 m s^{-1} at 2 m height. Based on measured 15 min time intervals, wind speeds high enough to potentially start erosion on bare fallow occurred at 13% during the observed period. This indicates limited wind speed events for potential wind erosion on bare fallow in the study area. In Central Asia, the wind speed increased significantly ($+0.6$ m s^{-1} decade^{-1}, $p < 0.001$) from 2011 to 2019, and moderate and heterogeneous changes are expected in future (Li et al., 2020; Wang et al., 2020). However, projections for northern Kazakhstan include particularly strong warmings and increasing precipitation that will also affect wind erosion severely, leading to complex spatiotemporal patterns (Li et al., 2020).

The disruptive force of water is another major factor causing the breakdown of aggregates, thus triggering soil erosion on cropland (Li & Fang, 2016). Applying three different wetting treatments simulating different field-relevant events of water-induced disruptions showed that all studied soils are at risk of water erosion. Depending on the applied wetting treatment, the erosion risk varies among soils, indicating that aggregate stability is ultimately controlled by the properties of the soil and the amount of energy applied (Le Bissonnais, 2016, 1996b). The fast wetting treatment indicated a severe breakdown of aggregates for all cropland soils. This aligns with Le Bissonnais (2016, 1996b), who showed that fast wetting during heavy rain or snowmelt is highly disruptive because of the slaking effect, that is, the compression of air trapped inside aggregates upon wetting (Le Bissonnais, 2016, 1996b; Yoder, 1936). In contrast, the disruption by slow wetting, as during sustained light rainfall, is assumed to result from disproportional swelling of materials, while wet shaking treatment decreases the mechanical cohesion upon raindrop impact (Le Bissonnais, 2016, 1996b).

According to the World Meteorological Organisation (WMO, 2018), precipitation <2.5 mm h^{-1} is defined as light rain, 2.5–10 mm h^{-1} as moderate rain, and 10–50 mm h^{-1} as heavy rain. In the study area, precipitation was measured on 154 days (observed period: 07/01/2019–06/30/2020), accounting for a total of 245.4 mm. Overall, rain occurred predominantly as light rain (96.6%), and it seems that differential swelling could be an important mechanism for the breakdown of aggregates in the study area. Thus, during light rain events or as a consequence of raindrop impact, there is a "frequent" risk in all situations or a "variable" risk of water erosion depending on topographic and climatic conditions (ISO 10930, 2011). Especially soils on Site 3–7 with SOC contents <30 g kg^{-1} are prone to water erosion during rainfall. Besides repetitive snowmelt in spring, heavy rain events were recorded in September 2019 (10.0 mm h^{-1}) and February 2020 (10.5 mm h^{-1}), assuming an intense aggregate
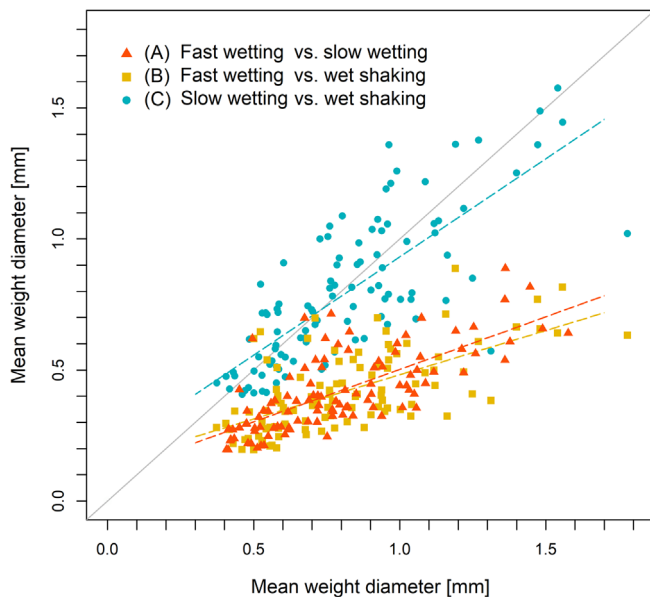
FIGURE 8 Scatterplot compares the three different wet-aggregate stability treatments with each other. The fast wetting treatment is the most disruptive test. In contrast, the MWDs obtained by slow wetting and wet shaking treatment are comparable. The positions of the dots to the 1:1 line indicate that the decline of aggregate stability between fast wetting and the other treatments increases with increasing MWD

breakdown and subsequent erosion by water runoff independent of the soil properties. However, the disruptive force of slaking during the heavy rain event under field conditions in September could be influenced by plant residues after harvesting (Six et al., 2004). In February, the soil temperature was still below the water freezing point and disruptive forces by water possibly interfered with structural changes induced by frost (Six et al., 2004).

Future model projections indicate a change in precipitation duration, magnitude, and intensity, causing an increase in rainfall erosivity in northern Kazakhstan (Duulatov et al., 2021). Based on an intermediate combined approach valuing duration and magnitude equally, Pruski and Nearing (2002) reported that every 1% of precipitation change could cause a 1.7% change in erosion. While currently all cropland soils in northern Kazakhstan are prone to disruptive forces by water, erosion might increase under higher precipitation rates in future, leaving the strongest negative impact on SOC-poor soils.

5 | CONCLUSIONS

Soil organic matter is the most important binding agent that supports aggregate stability in topsoils under grass- and cropland in semi-arid steppe regions. Tillage was not consistently accompanied by decreasing SOC content but always declined aggregate stability. We showed that soil properties, such as organic matter content and texture, determine the aggregate stability in a given soil. At the same time, tillage serves as an additional modifier enhancing the overall risk of wind and water erosion on all croplands. Nevertheless, erosion risk is generally higher for soils with low SOC content. Our results suggest that the aggregate stability of cropland soils in northern Kazakhstan is more vulnerable to the disruptive forces caused by water than by wind. The soil erodibility by wind is moderate, and wind speed conditions imply limited risk. In contrast, the breakdown of aggregates during wetting reveals a serious threat of water erosion. Even though the region is semi-arid, recurring heavy rain and snowmelt events imply a severe risk. Furthermore, disrupting aggregates by water may also promote subsequent soil loss by wind erosion. In particular, slacking during snowmelt potentially paves the way for extensive wind erosion in spring. The semi-arid steppe soils of Central Asia might face an even higher risk of combined water and wind erosion in future since predicted rainfall conditions might cause an increase in topsoil slacking. Therefore, sustainable land use strategies need to consider the potential risk of water erosion to mitigate further soil degradation.
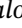
CONFLICT OF INTEREST
The authors declare no conflicts of interest.

DATA AVAILABILITY STATEMENT
The data that support the findings of this study are available from the corresponding author upon reasonable request.

ORCID
Moritz Koza https://orcid.org/0000-0002-7487-6668
Klaus Kaiser https://orcid.org/0000-0001-7376-443X
Robert Mikutta https://orcid.org/0000-0002-7186-6528
Christopher Conrad https://orcid.org/0000-0002-0807-7059
Cordula Vogel https://orcid.org/0000-0002-6525-2634
Kanat Akshalov https://orcid.org/0000-0003-2586-9944
Gerd Schmidt https://orcid.org/0000-0003-1557-5627

REFERENCES

Almaganbetov, N., & Grigoruk, V. (2008). Degradation of soil in Kazakhstan: Problems and challenges. In L. Simeonov & V. Sargsyan (Eds.), *Soil chemical pollution, risk assessment, remediation and security* (pp. 309–320). Springer. https://doi.org/10.1007/978-1-4020-8257-3_27

Almajmaie, A., Hardie, M., Acuna, T., & Birch, C. (2017). Evaluation of methods for determining soil aggregate stability. *Soil and Tillage Research*, *167*, 39–45. https://doi.org/10.1016/j.still.2016.11.003

Amézketa, E. (1999). Soil aggregate stability: A review. *Journal of Sustainable Agriculture*, *14*, 83–151. https://doi.org/10.1300/J064v14n02_08

Anderson, C. H., & Wenhardt, A. (1966). Soil erodibility, fall and spring. *Canadian Journal of Soil Science*, *46*, 255–259. https://doi.org/10.4141/cjss66-040

Robinson, S. (2016). Land degradation in Central Asia: Evidence, perception and policy. In: R. Behnke & M. Mortimore (Eds.), *The end of desertification?* (pp. 451–490). Springer. https://doi.org/10.1007/978-3-642-16014-1_17

Mirzabaev, A., Goedecke, J., Dubovyk, O., Djanibekov, U., Le, Q.B., Aw-Hassan, A. (2016). Economics of land degradation in Central Asia. In: E. Nkonya, A. Mirzabaev, & J. von Braun (Eds.), Economics of land degradation in Central Asia. In: *Economics of land degradation and improvement—A global assessment for sustainable development* (eds. Nkonya, E., Mirzabaev, A. & von Braun, J.), pp. 261–290. Springer International Publishing. https://doi.org/10.1007/978-3-319-19168-3_10

Bartoli, F., Hallett, P. D., & Cerdan, O. (2016). Le Bissonnais, Y. 1996. Aggregate stability and assessment of crustability and erodibility: 1. Theory and methodology. *European Journal of Soil Science*, *47*, 425–437. European Journal of Soil Science, 6. https://doi.org/10.1111/ejss.3_12311

Beniston, J. W., DuPont, S. T., Glover, J. D., Lal, R., & Dungait, J. A. J. (2014). Soil organic carbon dynamics 75 years after land-use change in perennial grassland and annual wheat agricultural systems. *Biogeochemistry*, *120*, 37–49. https://doi.org/10.1007/s10533-014-9980-3

Bischoff, N., Mikutta, R., Shibistova, O., Puzanov, A., Reichert, E., Silanteva, M., Grebennikova, A., Schaarschmidt, F., Heinicke, S., & Guggenberger, G. (2016). Land-use change under different climatic conditions: Consequences for organic matter and microbial communities in Siberian steppe soils. *Agriculture, Ecosystems & Environment*, *235*, 253–264. https://doi.org/10.1016/j.agee.2016.10.022

Bronick, C. J., & Lal, R. (2005). Soil structure and management: A review. *Geoderma*, *124*, 3–22. https://doi.org/10.1016/j.geoderma.2004.03.005

Caron, J., Espindola, C. R., & Angers, D. A. (1996). Soil structural stability during rapid wetting: Influence of land use on some aggregate properties. *Soil Science Society of America Journal*, *60*, 901–908. https://doi.org/10.2136/sssaj1996.03615995006000030032x

Cerdà, A., Flanagan, D. C., le Bissonnais, Y., & Boardman, J. (2009). Soil erosion and agriculture. *Soil and Tillage Research*, *106*, 107–108. https://doi.org/10.1016/j.still.2009.10.006

Chenu, C., Bissonnais, Y. L., & Arrouays, D. (2000). Organic matter influence on clay wettability and soil aggregate stability. *Soil Science Society of America Journal*, *64*, 1479–1486. https://doi.org/10.2136/sssaj2000.6441479x

Chepil, W. S. (1953). Field structure of cultivated soils with special reference to erodibility by wind. *Soil Science Society of America Proceedings*, *17*, 185–190.

Chepil, W. S. (1962). A compact rotary sieve and importance of dry sieving in physical soil analysis. *Soil Science Society of America Journal*, *26*, 4–6. https://doi.org/10.2136/sssaj1962.03615995002600010002x

Colazo, J. C., & Buschiazzo, D. E. (2010). Soil dry aggregate stability and wind erodible fraction in a semiarid environment of Argentina. *Geoderma*, *159*, 228–236. https://doi.org/10.1016/j.geoderma.2010.07.016

Cole, R. C. (1939). Soil macrostructure as affected by cultural treatment. *Hilgardia*, *12*, 427–472. https://doi.org/10.3733/hilg.v12n06p427

Diaz-Zorita, M., Perfect, E., & Grove, J. H. (2002). Disruptive methods for assessing soil structure. *Soil and Tillage Research*, *64*, 3–22. https://doi.org/10.1016/S0167-1987(01)00254-9

Dimoyiannis, D. G., Tsadilas, C. D., & Valmis, S. (1998). Factors affecting aggregate instability of Greek agricultural soils. *Communications in Soil Science and Plant Analysis*, *29*, 1239–1251. https://doi.org/10.1080/00103629809370023

Duulatov, E., Chen, X., Issanova, G., Orozbaev, R., Mukanov, Y., & Amanambu, A. C. (2021). *Current and Future Trends of Rainfall Erosivity and Soil Erosion in Central Asia*. Springer International Publishing. https://doi.org/10.1007/978-3-030-63509-1

Eynard, A., Schumacher, T., Lindstrom, M., & Malo, D. (2005). Effects of agricultural management systems on soil organic carbon in aggregates of Ustolls and Usterts. *Soil and Tillage Research*, *81*, 253–263. https://doi.org/10.1016/j.still.2004.09.012

FAO. (2012). *Aquastat: Kazakhstan*. Food and agriculture Organization of the United Nations (FAO).

FAO. (2014). *World reference base for soil resources 2014: International soil classification system for naming soils and creating legends for soil maps*. Food and Agriculture Organization of the United Nations (FAO).

Fernández-Ugalde, O., Virto, I., Barré, P., Gartzia-Bengoetxea, N., Enrique, A., Imaz, M. J., & Bescansa, P. (2011). Effect of carbonates on the hierarchical model of aggregation in calcareous semi-arid Mediterranean soils. *Geoderma*, *164*, 203–214. https://doi.org/10.1016/j.geoderma.2011.06.008

Frühauf, M., Meinel, T., & Schmidt, G. (2020). The virgin lands campaign (1954–1963) until the breakdown of the former Soviet Union (FSU): With special focus on western Siberia. In M. Frühauf, G. Guggenberger, T. Meinel, I. Theesfeld, & S. Lentz (Eds.), *KULUNDA: Climate smart agriculture* (pp. 101–118). Springer International Publishing. https://doi.org/10.1007/978-3-030-15927-6_8

Green, D. W., & Perry, R. H. (2007). *Perry's chemical engineers' handbook* (8th ed.). McGraw-Hill Professional Publishing.

Gyssels, G., Poesen, J., Bochet, E., & Li, Y. (2005). Impact of plant roots on the resistance of soils to erosion by water: A review. *Progress in Physical Geography: Earth and Environment*, *29*, 189–217. https://doi.org/10.1191/0309133305pp443ra

Hadas, A., & Wolf, D. (1984). Refinement and re-evaluation of the drop-shatter soil fragmentation method. *Soil and Tillage Research*, *4*, 237–249. https://doi.org/10.1016/0167-1987(84)90023-0

Hamidov, A., Helming, K., & Balla, D. (2016). Impact of agricultural land use in Central Asia: A review. *Agronomy for Sustainable Development*, *36*, 6. https://doi.org/10.1007/s13593-015-0337-7

Harris, I. C., Jones, P. D., & Osborn, T. (2020). CRU TS4.04: Climatic research unit (CRU) time-Series (TS) version 4.04 of high-resolution gridded data of month-by-month variation in climate (Jan. 1901-Dec. 2019). *Scientific Data*, *7*, 109.

Illiger, P., Schmidt, G., Walde, I., Hese, S., Kudrjavzev, A. E., Kurepina, N., Mizgirev, A., Stephan, E., Bondarovich, A., & Frühauf, M. (2019). Estimation of regional soil organic carbon stocks merging classified land-use information with detailed soil data. *Science of the Total Environment*, *695*, 133755. https://doi.org/10.1016/j.scitotenv.2019.133755

ISO 10930. (2011). *Soil quality—Measurement of the stability of soil aggregates subjected to the action of water*. International Organization for Standardization (ISO).

ISO 13320. (2009). *Particle size analysis—Laser diffraction methods*. International Organization for Standardization (ISO).

Jarvis, S., Tisdall, J., Oades, M., Six, J., Gregorich, E., & Kögel-Knabner, I. (2012). Landmark papers. *European Journal of Soil Science*, *63*, 1–21. https://doi.org/10.1111/j.1365-2389.2011.01408.x

Kassambara, A., Mundt, F. (2020). R package "factoextra": Extract and visualise the results of multivariate data analyses (version 1.0.7).

Kemper, W. D., & Rosenau, R. C. (2018). Aggregate stability and size distribution. In A. Klute (Ed.), *SSSA Book Series* (pp. 425–442). Soil Science Society of America, American Society of Agronomy. https://doi.org/10.2136/sssabookser5.1.2ed.c17

Koza, M., Schmidt, G., Bondarovich, A., Akshalov, K., Conrad, C., & Pöhlitz, J. (2021). Consequences of chemical pre-treatments in particle size analysis for modelling wind erosion. *Geoderma*, *396*, 115073. https://doi.org/10.1016/j.geoderma.2021.115073

Larney, F. (2007). Dry-aggregate size distribution. In M. Carter & E. Gregorich (Eds.), *Soil sampling and methods of analysis* (2nd ed., pp. 821–831). CRC Press. https://doi.org/10.1201/9781420005271.ch63

Le Bissonnais, Y. (1996a). Soil characteristics and aggregate stability. In M. Agassi (Ed.), *Soil erosion, conservation, and rehabilitation* (pp. 41–60). CRC Press.

Le Bissonnais, Y. (1996b). Aggregate stability and assessment of soil crustability and erodibility: I. Theory and methodology. *European Journal of Soil Science*, *47*, 425–437. https://doi.org/10.1111/j.1365-2389.1996.tb01843.x

Le Bissonnais, Y. (2016). Aggregate stability and assessment of soil crustability and erodibility: I. Theory and methodology. *European Journal of Soil Science*, *67*, 11–21. https://doi.org/10.1111/ejss.4_12311

Leys, J., Koen, T., & McTainsh, G. (1996). The effect of dry aggregation and percentage clay on sediment flux as measured by a portable field wind tunnel. *Soil Research*, *34*, 849. https://doi.org/10.1071/SR9960849

Li, J., Ma, X., & Zhang, C. (2020). Predicting the spatiotemporal variation in soil wind erosion across Central Asia in response to climate change in the 21st century. *Science of the Total Environment*, *709*, 136060. https://doi.org/10.1016/j.scitotenv.2019.136060

Li, J., Okin, G. S., & Epstein, H. E. (2009). Effects of enhanced wind erosion on surface soil texture and characteristics of windblown sediments: Wind erosion and soil characteristics. *Journal of Geophysical Research: Biogeosciences*, *114*, G02003. https://doi.org/10.1029/2008JG000903

Li, Z., & Fang, H. (2016). Impacts of climate change on water erosion: A review. *Earth-Science Reviews*, *163*, 94–117. https://doi.org/10.1016/j.earscirev.2016.10.004

López, M. V., de Dios Herrero, J. M., Hevia, G. G., Gracia, R., & Buschiazzo, D. E. (2007). Determination of the wind-erodible fraction of soils using different methodologies. *Geoderma*, *139*, 407–411. https://doi.org/10.1016/j.geoderma.2007.03.006

Malobane, M. E., Nciizah, A. D., Bam, L. C., Mudau, F. N., & Wakindiki, I. I. C. (2021). Soil microstructure as affected by tillage, rotation and residue management in a sweet sorghum-based cropping system in soils with low organic carbon content in South Africa. *Soil and Tillage Research*, *209*, 104972. https://doi.org/10.1016/j.still.2021.104972

Marshall, T., & Quirk, J. (1950). Stability of structural aggregates of dry soil. *Australian Journal of Agricultural Research*, *1*, 266. https://doi.org/10.1071/AR9500266

Mikhailova, E. A., Bryant, R. B., Vassenev, I. I., Schwager, S. J., & Post, C. J. (2000). Cultivation effects on soil carbon and nitrogen contents at depth in the russian Chernozem. *Soil Science Society of America Journal*, *64*, 738–745. https://doi.org/10.2136/sssaj2000.642738x

Moeys, J. (2018). *The soil texture wizard: R functions for plotting, classifying, transforming and exploring soil texture data*. Retrieved from https://cran.r-project.org/web/packages/soiltexture/vignettes/soiltexture_vignette.pdf.

Muñoz Sabater, J. (2019). *ERA5-land monthly averaged data from 1981 to present*. Copernicus Climate Change Service (C3S) Climate Data Store (CDS). https://doi.org/10.24381/CDS.68D2BB30

Nimmo, J. R., & Perkins, K. S. (2002). 2.6 Aggregate stability and size distribution. In J. H. Dane & G. Clarke Topp (Eds.), *SSSA book series* (pp. 317–328). Soil Science Society of America. https://doi.org/10.2136/sssabookser5.4.c14

Prishchepov, A. V., Schierhorn, F., Dronin, N., Ponkina, E. V., & Müller, D. (2020). 800 years of agricultural land-use change in asian (eastern) Russia. In M. Frühauf, G. Guggenberger, T. Meinel, I. Theesfeld, & S. Lentz (Eds.), *KULUNDA: Climate smart agriculture* (pp. 67–87). Springer International Publishing. https://doi.org/10.1007/978-3-030-15927-6_6

Pruski, F. F., & Nearing, M. A. (2002). Runoff and soil-loss responses to changes in precipitation: A computer simulation study. *Journal of Soil and Water Conservation*, *57*, 7–16.

R Core Team. (2020). *A language and environment for statistical computing*. R Foundation of Statistical Computing.

Rahmati, M., Eskandari, I., Kouselou, M., Feiziasl, V., Mahdavinia, G. R., Aliasgharzad, N., & McKenzie, B. M. (2020). Changes in soil organic carbon fractions and residence time

five years after implementing conventional and conservation tillage practices. *Soil and Tillage Research*, *200*, 104632. https://doi.org/10.1016/j.still.2020.104632

Reyer, C. P. O., Otto, I. M., Adams, S., Albrecht, T., Baarsch, F., Cartsburg, M., Coumou, D., Eden, A., Ludi, E., Marcus, R., Mengel, M., Mosello, B., Robinson, A., Schleussner, C.-F., Serdeczny, O., & Stagl, J. (2017). Climate change impacts in Central Asia and their implications for development. *Regional Environmental Change*, *17*, 1639–1650. https://doi.org/10.1007/s10113-015-0893-z

Reynolds, J. F., Smith, D. M. S., Lambin, E. F., Turner, B. L., Mortimore, M., Batterbury, S. P. J., Downing, T. E., Dowlatabadi, H., Fernández, R. J., Herrick, J. E., Huber-Sannwald, E., Jiang, H., Leemans, R., Lynam, T., Maestre, F. T., Ayarza, M., & Walker, B. (2007). Global desertification: Building a science for dryland development. *Science*, *316*, 847–851. https://doi.org/10.1126/science.1131634

Scheffer, F., Schachtschabel, P., & Blume, H.-P. (2016). *Soil science* (1st ed.). Springer.

Schmidt, G., Illiger, P., Kudryavtsev, A. E., Bischoff, N., Bondarovich, A. A., Koshanov, N. A., & Rudev, N. V. (2020). Physical soil properties and erosion. In M. Frühauf, G. Guggenberger, T. Meinel, I. Theesfeld, & S. Lentz (Eds.), *KULUNDA: Climate smart agriculture* (pp. 155–166). Springer International Publishing. https://doi.org/10.1007/978-3-030-15927-6_11

Shao, Y. (2008). *Physics and modelling of wind erosion*. Springer, Cambridge. https://doi.org/10.1007/978-1-4020-8895-7

Shiyatyi, E. I. (1965). Wind structure and velocity over a rugged soil surface. Bulletin of Agriculture, 10 (in Russian) Cited by Zachar, D. (1982). Erosion factors and conditions governing soil erosion and erosion processes. In *Soil erosion* (pp. 205–387). Elsevier.

Six, J., Bossuyt, H., Degryze, S., & Denef, K. (2004). A history of research on the link between (micro)aggregates, soil biota, and soil organic matter dynamics. *Soil and Tillage Research*, *79*, 7–31. https://doi.org/10.1016/j.still.2004.03.008

Six, J., Elliott, E. T., Paustian, K., & Doran, J. W. (1998). Aggregation and soil organic matter accumulation in cultivated and native grassland soils. *Soil Science Society of America Journal*, *62*, 1367–1377. https://doi.org/10.2136/sssaj1998.03615995006200050032x

Skidmore, E. L., Hagen, L. J., Armbrust, D. V., Durar, A. A., Fryrear, D. W., Potter, K. N., Wagner, L. E., & Zobeck, T. M. (1994). In R. Lal (Ed.), *Soil erosion, research methods* (2nd ed., pp. 295–330). St. Lucie Press.

Soil Science Division Staff (2017). Soil survey manual. In C. Ditzler, K. Scheffe, & H. C. Monger (Eds.), *Handbook 18*. Government Printing Office Retrieved from https://www.nrcs.usda.gov/wps/portal/nrcs/detailfull/soils/ref/?cid=nrcs142p2_054262

Stolbovoi, V. (2000). *Soils of Russia: Correlated with the revised legend of the FAO soil map of the world and world Reference Base for soil resources*. International Institute for Applied Systems Analysis.

Suarez, D. L. (2017). Inorganic carbon: Land use impacts. In R. Lal (Ed.), *Encyclopedia of soil science* (3rd ed., p. 1210). CRC Press. https://doi.org/10.1081/E-ESS3-120001765

Taiyun, W., Simko, V. (2021). R package "corrplot": Visualisation of a correlation matrix (version 0.92).

Teixeira, E. I., Fischer, G., van Velthuizen, H., Walter, C., & Ewert, F. (2013). Global hot-spots of heat stress on agricultural crops due to climate change. *Agricultural and Forest Meteorology*, *170*, 206–215. https://doi.org/10.1016/j.agrformet.2011.09.002

Tisdall, J. M., & Oades, J. M. (1982). Organic matter and water-stable aggregates in soils. *European Journal of Soil Science*, *33*, 141–163. https://doi.org/10.1111/j.1365-2389.1982.tb01755.x

Uspanov, U.U., Yevstifeyev, U.G., Storozhenko, D.M., Lobova, E.V. (1975). Soil map of the kazakh SSR 1:2.500.000.

Virto, I., Gartzia-Bengoetxea, N., & Fernández-Ugalde, O. (2011). Role of organic matter and carbonates in soil aggregation estimated using laser diffractometry. *Pedosphere*, *21*, 566–572. https://doi.org/10.1016/S1002-0160(11)60158-6

Wang, W., Samat, A., Ge, Y., Ma, L., Tuheti, A., Zou, S., & Abuduwaili, J. (2020). Quantitative soil wind erosion potential mapping for Central Asia using the Google earth engine platform. *Remote Sensing*, *12*, 3430. https://doi.org/10.3390/rs12203430

WHO. (2012). *Capacity of the health system in Kazakhstan for crisis management: Kazakhstan, 2010*. World Health Organization, Regional Office for Europe.

Wieringa, J. (1992). Updating the Davenport roughness classification. *Journal of Wind Engineering and Industrial Aerodynamics*, *41*, 357–368. https://doi.org/10.1016/0167-6105(92)90434-C

WMO. (2018). *Guide to meteorological instruments and methods of observation*. World Meteorological Organization.

Woche, S. K., Goebel, M.-O., Mikutta, R., Schurig, C., Kaestner, M., Guggenberger, G., & Bachmann, J. (2017). Soil wettability can be explained by the chemical composition of particle interfaces—An XPS study. *Scientific Reports*, *7*, 42877. https://doi.org/10.1038/srep42877

Xue, B., Huang, L., Huang, Y., Zhou, F., Li, F., Kubar, K. A., Li, X., Lu, J., & Zhu, J. (2019). Roles of soil organic carbon and iron oxides on aggregate formation and stability in two paddy soils. *Soil and Tillage Research*, *187*, 161–171. https://doi.org/10.1016/j.still.2018.12.010

Yoder, R. E. (1936). A direct method of aggregate analysis of soils and a study of the physical nature of erosion losses. *Agronomy Journal*, *28*, 337–351. https://doi.org/10.2134/agronj1936.00021962002800050001x

Zachar, D. (1982). Erosion factors and conditions governing soil erosion and erosion processes. In *Soil erosion* (pp. 205–387). Elsevier. https://doi.org/10.1016/S0166-2481(08)70647-0

Zepner, L., Karrasch, P., Wiemann, F., & Bernard, L. (2021). ClimateCharts.net—An interactive climate analysis web platform. *International Journal of Digital Earth*, *14*(3), 338–356. https://doi.org/10.1080/17538947.2020.1829112

APPENDIX A

TABLE A1 Mean values of soil properties for all plots from each site under both land use types (grassland, grass; cropland, crop). Lower case letters indicate statistical significances ($p < 0.05$); MWD refers to the mean weight diameter

Site(s)	Land-use type	n	pH [-]	Electrical conductivity [µS cm⁻¹]	Total inorganic carbon [g kg⁻¹]	Soil organic carbon [g kg⁻¹]	Clay [%]	Silt [%]	Sand [%]	Drop-shatter MWD [mm]	Fast wetting MWD [mm]	Slow wetting MWD [mm]	Wet shaking MWD [mm]
1	Grass	1	6.7 b	167.0 b	0.1 ab	47.6 a	18.9 a	76.0 a	5.1 b	12.0 a	2.0 a	2.6 a	2.2 a
	Crop	4	6.5 b	306.0 ab	0.4 a	36.6 b	22.1 a	50.7 b	27.2 a	6.1 b	0.5 b	1.2 b	1.2 b
	Crop	4	7.6 a	481.0 a	0.1 b	36.0 b	25.1 a	65.9 a	9.0 b	7.5 b	0.4 b	1.1 b	1.2 b
2	Grass	4	8.3 a	564.0 a	0.9 bc	40.0 a	21.1 b	74.7 a	4.2 b	12.0 a	1.8 a	2.5 a	1.8 a
	Crop	4	7.1 b	336.5 a	0.1 c	34.9 a	24.6 ab	63.4 bcd	12.0 ab	9.9 ab	0.6 b	1.1 bc	0.9 bc
	Crop	4	7.4 ab	412.8 a	0.4 c	33.7 a	22.7 ab	55.6 d	21.8 a	9.5 ab	0.6 b	1.1 bc	1.0 bc
	Crop	4	7.7 ab	419.5 a	2.9 ac	32.8 a	27.8 a	60.5 cd	11.7 ab	8.3 bc	0.6 b	1.0 bc	0.9 bc
	Crop	4	7.7 ab	396.8 a	2.6 ab	32.9 a	23.8 ab	69.2 abc	7.0 b	5.1 c	0.4 b	0.9 bc	0.7 bc
	Crop	4	7.4 ab	364.3 a	0.1 c	34.3 a	21.3 b	72.2 ab	6.5 b	6.0 c	0.5 b	1.2 b	1.1 b
	Crop	4	7.7 ab	423.8 a	1.9 abc	32.1 a	25.5 ab	62.6 bcd	12.0 ab	7.8 bc	0.4 b	0.7 c	0.7 c
3	Grass	4	7.9 a	196.3 b	3.5 c	28.2 a	20.5 a	71.9 a	7.6 a	7.7 a	1.0 a	1.9 a	1.6 a
	Crop	4	7.9 a	242.5 b	5.2 ab	19.8 b	21.1 a	71.7 a	7.2 a	4.8 a	0.4 ab	0.8 b	0.9 a
	Crop	4	7.9 a	375.3 a	5.4 a	19.2 b	21.8 a	72.5 a	5.7 a	3.5 a	0.4 ab	0.7 b	0.8 b
	Crop	4	8.0 a	213.0 b	5.2 ab	19.7 b	24.3 a	68.1 a	7.6 a	5.0 a	0.3 ab	0.6 b	0.7 b
	Crop	4	7.9 a	174.3 b	4.1 bc	19.1 b	21.6 a	70.3 a	8.1 a	5.3 a	0.3 b	0.7 b	0.7 b
4	Grass	4	6.3 b	384.0 a	0.1 b	27.0 a	12.3 b	45.0 b	42.7 a	8.4 a	1.2 a	2.2 a	1.8 a
	Crop	4	7.0 ab	392.3 a	0.2 b	27.5 a	19.1 ab	55.8 ab	25.1 ab	6.8 ab	0.4 b	0.8 b	0.8 b
	Crop	4	8.3 a	353.3 a	4.4 a	23.4 a	21.2 a	66.9 a	11.9 b	4.9 b	0.4 b	0.7 b	0.6 b
	Crop	4	6.3 b	310.3 a	0.1 b	21.0 a	18.6 ab	51.1 ab	30.3 ab	6.6 ab	0.2 b	0.5 b	0.5 b
	Crop	4	6.7 ab	311.3 a	0.6 b	27.6 a	19.0 a	54.8 ab	26.3 ab	7.0 ab	0.5 b	0.7 b	0.7 b
5	Grass	4	7.1 b	147.8 b	0.1 b	25.3 a	16.0 a	59.9 b	24.1 a	6.2 a	1.0 a	2.0 a	1.4 a
	Crop	4	7.9 a	266.3 a	7.4 a	16.5 b	19.0 a	69.1 ab	11.9 ab	4.6 b	0.3 b	0.7 b	0.9 b
	Crop	4	8.2 a	231.0 ab	7.5 a	17.5 ab	19.2 a	65.1 ab	15.7 ab	4.6 b	0.3 b	0.6 b	0.7 b
6	Grass	4	6.7 a	64.8 a	0.1 a	13.5 a	10.2 a	35.7 a	54.1 a	10.0 a	1.4 a	1.4 a	1.6 a
	Crop	4	7.2 a	355.5 a	0.2 a	11.5 a	17.8 a	50.8 a	31.4 a	2.5 b	0.5 b	0.7 a	0.7 a
	Crop	4	7.4 a	160.0 a	0.2 a	12.9 a	19.9 a	49.0 a	31.1 a	4.1 b	0.7 b	1.2 a	1.4 a

(Continues)

TABLE A1 (Continued)

Site(s)	Land-use type	n	pH [-]	Electrical conductivity [$\mu S\,cm^{-1}$]	Total inorganic carbon [$g\,kg^{-1}$]	Soil organic carbon [$g\,kg^{-1}$]	Clay [%]	Silt [%]	Sand [%]	Drop-shatter MWD [mm]	Fast wetting MWD [mm]	Slow wetting MWD [mm]	Wet shaking MWD [mm]
	Crop	4	7.3 [a]	170.5 [a]	0.2 [a]	14.2 [a]	17.2 [a]	44.9 [a]	37.9 [a]	4.7 [b]	0.6 [b]	0.8 [a]	1.0 [a]
	Crop	4	7.2 [a]	108.5 [a]	0.1 [a]	14.5 [a]	19.6 [a]	51.5 [a]	28.8 [a]	6.8 [ab]	0.6 [b]	0.8 [a]	1.1 [a]
7	Grass	4	6.5 [b]	49.0 [b]	0.1 [a]	15.3 [a]	7.8 [a]	34.8 [a]	57.3 [a]	11.0 [a]	0.7 [a]	1.5 [a]	0.9 [a]
	Crop	4	7.3 [a]	134.5 [ab]	0.3 [a]	16.2 [a]	9.5 [a]	35.0 [a]	55.5 [a]	3.6 [c]	0.4 [b]	0.6 [b]	0.5 [b]
	Crop	4	6.4 [b]	138.8 [a]	0.1 [a]	11.6 [a]	9.3 [a]	32.5 [a]	57.8 [a]	6.7 [b]	0.3 [b]	0.5 [b]	0.5 [b]
	Crop	4	6.5 [b]	70.8 [ab]	0.1 [a]	13.1 [a]	10.9 [b]	36.1 [a]	53.0 [a]	3.4 [c]	0.3 [b]	0.5 [b]	0.5 [b]
	Crop	4	6.7 [b]	61.5 [ab]	0.1 [a]	14.2 [a]	11.6 [a]	45.9 [a]	42.5 [a]	5.7 [bc]	0.3 [b]	0.5 [b]	0.6 [b]

TABLE A2 Correlation coefficients (r) between aggregate stabilities and soil properties with statistical significances levels ($p < 0.001 =$ ***, $p < 0.01 =$ **, $p < 0.05 =$ *) for all sites

Site(s)	Aggregate stability indicators	pH r^p	Electrical conductivity r^p	Total inorganic carbon r^p	Soil organic carbon r^p	Clay r^p	Silt r^p	Sand r^p
All	Drop-shatter	−0.20 *	0.12	−0.27 **	0.51 ***	0.10	0.06	−0.08
	Fast wetting	−0.11	0.05	−0.27 **	0.42 ***	−0.04	0.15	−0.10
	Slow wetting	−0.09	0.09	−0.25 **	0.49 ***	0.00	0.19 *	−0.14
	Wet shaking	−0.07	0.06	−0.18 *	0.43 ***	0.12	0.26 **	−0.23 **
1	Drop-shatter	−0.16	−0.55	−0.17	0.76 **	−0.53	0.78 **	−0.65 *
	Fast wetting	−0.37	−0.69 *	−0.24	0.81 **	−0.63 *	0.68 *	−0.50
	Slow wetting	−0.33	−0.74 **	−0.22	0.77 **	−0.51	0.67 *	−0.53
	Wet shaking	−0.21	−0.65 *	−0.19	0.77 **	−0.56	0.74 **	−0.59 *
2	Drop-shatter	0.01	0.17	−0.27	0.30	−0.04	−0.27	0.29
	Fast wetting	0.57 **	0.52 **	−0.12	0.22 *	−0.28	0.36	−0.25
	Slow wetting	0.45 *	0.44 *	−0.21	0.38 **	−0.36	0.38	−0.24
	Wet shaking	0.31	0.34	−0.28	0.40 **	−0.32	0.40 *	−0.27
3	Drop-shatter	0.21	−0.33	−0.43 **	0.35 ***	0.13	−0.18	0.15
	Fast wetting	−0.20	-0.05	−0.64 **	0.77 ***	−0.09	0.19	−0.25
	Slow wetting	−0.10	−0.19	−0.67 **	0.83 ***	−0.21	0.23	−0.10
	Wet shaking	−0.16	−0.07	−0.59 **	0.77 ***	−0.12	0.18	−0.17
4	Drop-shatter	−0.61 **	0.20	−0.38	0.48 *	−0.28	−0.43	0.40
	Fast wetting	−0.37	0.20	−0.21	0.25	−0.55	−0.31 *	0.39
	Slow wetting	−0.32	0.37	−0.23	0.24	−0.60	−0.34 **	0.42
	Wet shaking	−0.34	0.32	−0.22	0.21	−0.59	−0.36 **	0.43
5	Drop-shatter	−0.62 *	−0.09	−0.38	0.52	0.15	−0.55	0.40
	Fast wetting	−0.85 ***	−0.60 *	−0.86 ***	0.85 ***	−0.53	−0.52	0.61 *
	Slow wetting	−0.89 ***	−0.57	−0.92 ***	0.87 ***	−0.59 *	−0.54	0.64 *
	Wet shaking	−0.78 **	−0.50	−0.73 **	0.75 **	−0.51	−0.35	0.47
6	Drop-shatter	−0.02	−0.27	-0.12	0.38	−0.02	−0.05	0.04
	Fast wetting	−0.01	−0.22	−0.16	0.05	−0.21 *	−0.40 **	0.36 **
	Slow wetting	0.12	−0.20	−0.09	0.12	0.01	−0.25	0.18
	Wet shaking	−0.02	−0.41	−0.30	0.41	0.26	0.04	−0.12
7	Drop-shatter	−0.42	−0.32	−0.22	0.07	−0.27	0.01	0.05
	Fast wetting	0.03	−0.20	−0.16	0.16	−0.53 *	−0.27	0.35
	Slow wetting	−0.05	−0.33	−0.19	0.26	−0.41	−0.11	0.19
	Wet shaking	−0.18	−0.17	−0.28	0.43	−0.13	0.24	−0.16

TABLE A3 Soil properties of all sites and both land use types (grassland, grass; cropland, crop)

Site(s)	Land-use type(s)	n	pH [-]	Electrical conductivity [µS cm⁻¹]	Total inorganic carbon [g kg⁻¹]	Soil organic carbon [g kg⁻¹]	Clay [%]	Silt [%]	Sand [%]	Drop-shatter MWD [mm]	Fast wetting MWD [mm]	Slow wetting MWD [mm]	Wet shaking MWD [mm]
All	Both	132	7.3±0.8	261.9±158.3	1.7±2.3	23.9±10.9	18.8±5.7	57.3±14.4	23.9±18.9	6.6±3.0	0.6±0.5	1.0±0.6	1.0±0.5
	Grass	28	7.1±0.8	198.6±162.5	0.7±1.2	28.1±13.9	15.3±5.4	56.9±18.0	29.9±23.0	9.6±3.1	1.3±0.6	2.0±0.6	1.6±0.5
	Crop	104	7.3±0.8	277.8±144.3	2.5±1.2	22.8±9.6	19.8±5.4	57.4±13.3	17.5±1.3	5.8±2.4	0.4±0.2	0.8±0.3	0.8±0.3
1	Both	12	6.9±0.5	322.2±157.0	0.2±0.2	40.2±6.7	22.2±3.8	64.3±11.5	13.4±10.8	8.7±2.5	1.0±0.7	1.6±0.7	1.5±0.5
	Grass	4	6.7±0.3	167.0±58.1	0.1±0.1	47.6±4.9	18.9±3.0	76.0±2.3	5.1±2.4	12.0±0.0	2.0±0.2	2.6±0.1	2.2±0.1
	Crop	8	7.0±0.6	399.8±131.3	0.2±0.2	36.4±3.6	23.9±2.9	58.5±9.6	17.6±10.9	7.0±1.1	0.5±0.1	1.1±0.2	1.2±0.2
2	Both	32	7.6±0.5	405.5±126.0	1.3±1.3	34.4±6.1	23.8±3.0	65.4±7.6	10.7±7.4	8.4±2.5	0.6±0.5	1.2±0.5	1.0±0.3
	Grass	4	8.3±0.8	564.0±382.0	0.9±0.6	40.0±14.3	21.1±1.3	74.7±4.0	4.2±3.1	12.0±0.0	1.8±0.3	2.5±0.2	1.8±0.1
	Crop	2S	7.5±0.3	392.3±52.6	1.3±1.4	33.5±1.9	24.3±2.9	63.9±6.9	11.8±7.4	7.7±2.2	0.5±0.1	1.0±0.2	0.9±0.2
3	Both	20	7.9±0.1	240.3±79.2	4.7±0.9	21.2±4.1	21.9±2.7	70.9±3.0	7.2±1.3	5.3±3.1	0.5±0.4	0.9±0.6	0.9±0.4
	Grass	4	7.9±0.1	196.3±27.0	3.5±0.8	28.2±4.4	20.5±1.8	71.9±1.3	7.6±1.5	7.7±4.3	1.0±0.6	1.9±0.6	1.6±0.6
	Crop	16	7.9±0.1	251.3±83.9	5.0±0.6	19.5±0.8	22.2±2.8	70.7±3.3	7.1±1.2	4.7±2.4	0.3±0.1	0.7±0.1	0.8±0.1
4	Both	20	6.9±1.1	350.2±94.5	1.1±1.9	25.3±10.3	18.0±3.8	54.7±10.3	27.3±13.6	6.7±1.8	0.5±0.4	1.0±0.7	0.9±0.6
	Grass	4	6.3±0.7	384.0±115.3	0.1±0.0	27.0±11.6	12.3±2.4	45.0±6.1	42.7±8.4	8.4±2.2	1.2±0.4	2.2±0.6	1.8±0.5
	Crop	16	7.1±1.1	341.8±86.5	1.3±2.0	24.9±9.9	19.5±2.4	57.1±9.7	23.4±11.8	6.3±1.4	0.4±0.1	0.7±0.2	0.6±0.2
5	Both	12	7.7±0.5	215.0±66.1	5.0±3.6	19.8±5.4	18.1±2.1	64.7±5.0	17.2±6.1	5.1±1.8	0.5±0.4	1.1±0.7	1.0±0.4
	Grass	4	7.1±0.2	147.8±65.2	0.1±0.0	25.3±6.3	16.0±1.9	59.9±2.9	24.1±3.9	6.2±0.8	1.0±0.3	2.0±0.4	1.4±0.3
	Crop	8	8.0±0.3	248.6±32.1	7.4±0.9	17.0±1.0	19.1±1.2	67.1±4.0	13.8±3.4	4.6±1.9	0.3±0.0	0.6±0.1	0.8±0.2
6	Both	20	7.2±0.9	171.9±176.3	0.2±0.2	13.3±3.2	17.0±5.3	46.4±10.8	36.6±15.3	5.6±3.3	0.7±0.3	1.0±0.4	1.1±0.4
	Grass	4	6.7±0.5	64.8±28.5	0.1±0.1	13.5±3.5	10.2±3.8	35.7±11.0	54.1±13.9	10.0±3.4	1.4±0.1	1.4±0.5	1.6±0.5
	Crop	16	7.3±0.9	198.6±187.2	0.2±0.2	13.3±3.2	18.7±4.2	49.0±9.0	32.3±12.2	4.5±2.2	0.6±0.1	0.9±0.3	1.1±0.4
7	Both	20	6.7±0.4	90.9±51.9	0.1±0.2	14.1±2.9	9.8±2.6	36.9±8.8	53.2±10.9	6.1±2.9	0.4±0.2	0.7±0.4	0.6±0.2
	Grass	4	6.5±0.1	49.0±20.0	0.1±0.0	15.3±2.9	7.8±1.9	34.8±9.0	57.3±10.9	11.0±1.8	0.7±0.0	1.5±0.1	0.9±0.2
	Crop	16	6.7±0.4	101.4±52.1	0.1±0.2	13.8±2.8	10.3±2.5	37.4±8.7	52.2±10.6	4.8±1.6	0.3±0.1	0.5±0.1	0.5±0.1

Note: Values are shown as arithmetic means ± SD; MWD refers to the mean weight diameter.